Reversible Fragmentation and Self-Assembling of Nematic Liquid Crystal Droplets on Functionalized Pyroelectric Substrates

Francesco Merola, Simonetta Grilli, Sara Coppola, Veronica Vespini, Sergio De Nicola, Pasquale Maddalena, Cosimo Carfagna, and Pietro Ferraro*

Investigation on the behavior of nematic liquid crystals on functionalized polar dielectric crystal substrates is accomplished. Very interesting effects can be observed in maneuvering liquid crystal droplets on the substrate surface, driven by electric fields generated by pyroelectric effect. Reversible drops fragmentation and self-assembling in different configurations can be achieved. The dynamics of the observed phenomena is studied and the repeatability of the process is full assessed.

1. Introduction

Liquid crystals (LCs) find wide applicability in many fields ranging from display systems as well as in optics and photonics.[1–9] The major attractive feature of LCs lies in the fact that their optical properties can be modulated by electric, optical or magnetic fields. At present, many issues are still open and further developments for manipulating and dynamically control LCs are highly demanding in many emerging fields of technology but also in fundamental research. For example LC tunable lenses have been extensively studied and many successful configurations have been designed and experimentally demonstrated.[10–13] Optical microresonators[14] and unique optical elements for quantum cloning of orbital angular momentum photon qubits[15] have been developed. LC based optical devices such as electro-optic switches and beam scanners have been proposed for application in managing radiation and imaging in THz region.[16–18]

In many of these proposed devices, the delivering of liquid crystals is accomplished by ink-jet printing methods, but efficient alternatives could be the spatial self-assembly of LC drops.

On the other side, ferroelectric and/or pyroelectric crystals are widely studied and employed for patterning or assembling organic and inorganic structures,[19–25] also displaying different behaviors depending on the sign of the charged surface.[26] In particular, lithium niobate (LN) finds applications as selective decoration of LN domains by polystyrene microspheres,[22] fabrication of silver nanowires on LN domain boundaries,[27] as well as Ag deposition on periodically poled LN (PPLN)[28] and deposition of different elemental metals confined to the ferroelectric LN domain walls.[29]

Furthermore, combination of photonics properties of LN with LC electro-optics could be also provided if taking into account the recent advancements for LN crystal in photonics.[30]

Lately, a novel approach has been discovered for manipulating different classes of liquids by exploiting the pyroelectric effect, where the strong electric fields pyroelectrically generated allow to manipulate liquids in 2D on a substrate or even in 3D for dispensing liquids from one liquid reservoir to a dispensable substrate. Among various applications demonstrated by taking advantage of this effect we cite spatial modulation of the wettability (i.e., wettability patterning), fabrication of arrays of solid polymeric microlenses, realization of arrays of tunable liquid lenses, and finally liquid dispensing, patterning and curing at nanoscale.[31–36]

In this paper the behavior of LC droplets on z-cut LN wafers is reported.[37,38] The LN sample is functionalized in various configurations, in particular by micro-engineering its ferroelectric domains (i.e. by spatially arranging the inverted ferroelectric domains) and covering its surface with a film of hydrophobic polymer. Very promising effects are reported and discussed. Essentially, a reversible uniform fragmentation of large LC drops has been observed.[39–45] In fact, driven by the pyroelectric fields obtained by a thermal stimulus applied to the LN substrate, the fragmented drops are self-assembled on the substrate according to the underneath ferroelectric domain patterned structures into LN. Successive coalescence of the fragmented tiny drops is observed on a longer time scale. Reversible character of the whole process has been verified. The aforementioned phenomena are deeply investigated

---

Dr. F. Merola, Dr. S. Grilli, Dr. S. Coppola,
Dr. V. Vespini, Dr. S. De Nicola, Dr. P. Ferraro
Istituto Nazionale di Ottica (CNR-INO)
Via Campi Flegrei 34, 80078 Pozzuoli (NA), Italy
E-mail: francesco.merola@ino.it
Dr. S. Coppola
Università degli Studi di Napoli "Federico II"
Piazzale Tecchio 80, 80125 Napoli, Italy
Prof. P. Maddalena
Università degli Studi di Napoli "Federico II"
Dipartimento di Scienze Fisiche
Via Cintia, 80126 Napoli, Italy
Prof. C. Carfagna
Istituto di Chimica e Tecnologia dei Polimeri (CNR-ICTP)
Via Campi Flegrei 34, 80078 Pozzuoli (NA), Italy

DOI: 10.1002/adfm.201200323

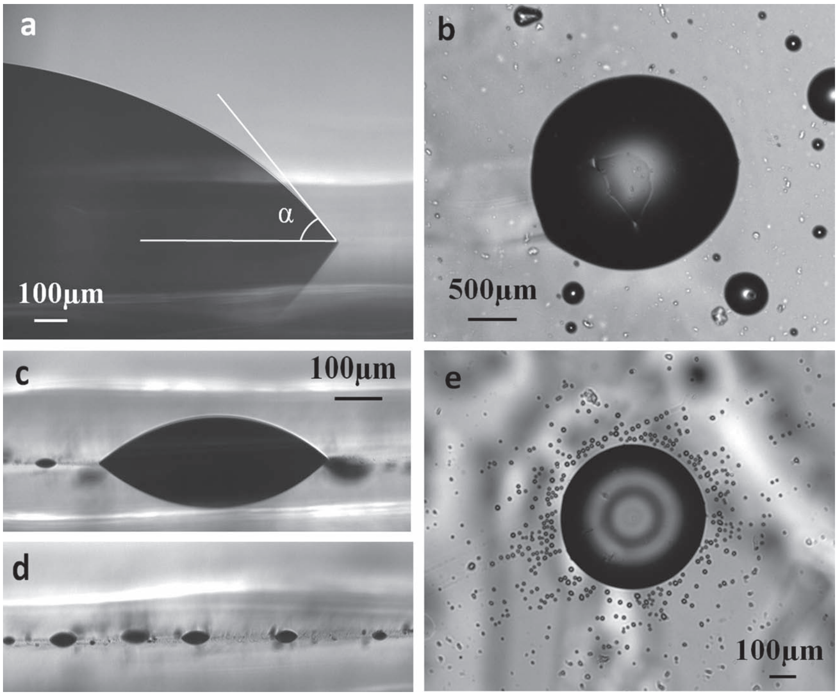

Figure 1. (a) Side and (b) top view of a big LC drop placed onto a PDMS substrate. The calculated contact angle is about 50°. (c-d) Side and (e) top view of the sample after heating: the big drop is fragmented in a "mother" drop (c) and "daughter" droplets (d).

and results of many experiments are shown in different configurations.

2. Liquid Crystal's Fragmentation and Self-Patterning

When deposited on a hydrophobic (i.e. non-wetting) substrate, a liquid thin film undergoes instability phenomena, mainly driven by inter-molecular forces (e.g. hydrogen bonds or van der Waals forces) and by variations of the surface tension with temperature or liquid composition.[46] The conditions for which these instabilities produce dewetting are governed by the interaction potential of the film, which describes the effective interaction between the solid-liquid interface and the liquid-air interface.[47] On the other side it is known, in some circumstances, the low hydrophobicity of the widely used polydimethylsiloxane (PDMS) polymer in contact with a nematic LC.[48]

Starting from these assumptions, the behavior of a nematic liquid crystal in contact with a PDMS substrate, subject to a temperature variation has been tested. It has to be said that, due to the PDMS non-full wettability, it is difficult to obtain a LC homogeneous thin layer upon it. Vice versa, the LC arranges itself in drops, with a relatively large contact angle, as shown in **Figure 1**(a-b). Thanks to the applied thermal input, a dewetting-like phenomenon occurs, in analogy with Sun et al.[45] The thermodynamic instability produces a fragmentation of the big drops into smaller droplets, with the "daughter" drops surrounding the "mother" one,[43–45] as displayed in Figure 1(c-e).

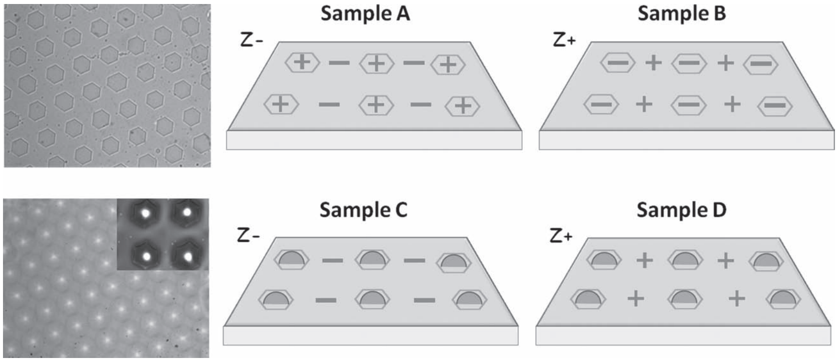

Figure 2. Fabricated samples. Sample A: PDMS flat film on PPLN Z- face; sample B: PDMS flat film on PPLN Z+ face; sample C: PDMS microlens array on PPLN Z- face; sample D: PDMS microlens array on PPLN Z+ face. The plus and minus represent the signs of the electric charges. On the left optical microscope images of the PDMS flat film on PPLN (first row) and PDMS microlens array (second row) are reported. The pitch of the structures is about 200 µm.

At this point we might ask: what would occur if under the PDMS layer, a geometrical structure was present, capable to drive these small droplets, that otherwise would be distributed on the substrate in a random configuration? The answer is very fascinating, and will be exposed in the following.

Experimental measurements are carried out on four different samples, that we named A,B,C and D, and represented in **Figure 2**. Details about the fabrication of all samples are given in the experimental section. In the following experiments a small quantity of nematic liquid crystal 1-(*trans*-4-Hexylcyclohexyl)-4-isothiocyanatobenzene,[49,50] abbreviated 6CHBT (with phase sequence Cr 12.5 °C N 43.2 °C I), from Sigma Aldrich, is placed onto each sample. This LC has been chosen for the polar structure of the molecule. The importance of this statement will be clear soon.

Successively, the sample is heated on a hot plate at 90 °C (above the nematic to isotropic transition temperature) for 30s and then placed at room temperature under an optical microscope in transmission configuration.

In the case of a PDMS film spin-coated onto the Z- face of a periodically poled lithium niobate (PPLN) substrate (sample A), the starting situation is that of many LC drops (with different dimensions) scattered all over the sample, as in Figure 3(a). On heating the specimen, a quite uniform fragmentation of the LC drops occurs; a high density of smaller droplets covers the whole sample, as reported in **Figure 3**(b) and (c). This phenomenon resembles the well-known dewetting effect.[31,46,47,51–55]

The behavior of the liquid crystal drops during the cooling step requires some further

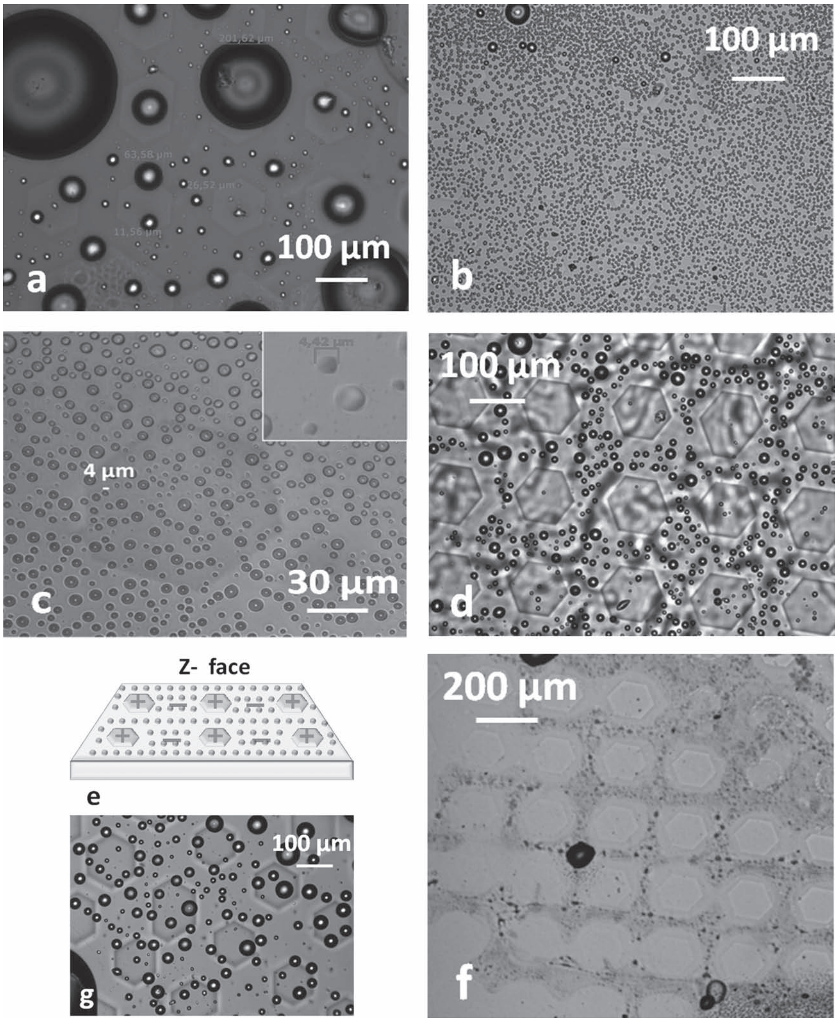

Figure 3. Temporal evolution of the experiment on sample A. (a) LC drops scattered on the sample without any geometry, before heating. Magnification is about 500. (b) First frame of Movie 1: fragmented LC droplets suddenly after heating at 90 °C, much smaller than before heating. LN hexagonal domains are not well visible, covered by the droplets. (c) Magnified view of (b). (d) Last frame of Movie 1 (2 hours after beginning of cooling) and (e) corresponding scheme. (f) Bigger field of view of (d). (g) Coalesced LC drops on the sample after some days at room temperature: the configuration is almost random as before heating.

analysis. For doing this, different images recorded at the microscope during cooling (with a room temperature of 22 °C) for two hours are reported. Figures 3(b) and (d) show two significant pictures from a dynamic recorded sequence (Movie 1), one at the beginning of cooling process (b) and the second 2 hours later (d). Figure 3(e) represents the scheme corresponding to Figure 3(d), while Figure 3(f) is a de-magnified view of Figure 3(d).

The first evidence is that almost all of the LC drops move selectively in the areas around the hexagons. The further significant aspect is that the fragmented drops gradually coalesce. After two hours, in fact, the average size of the drops is substantially increased (see Figure 3(d)). This phenomenon could be probably ascribed to a reduction of the interfacial tension between nematic LC and PDMS with the decreasing of temperature.[56]

Moreover, the process is reversible in the sense that after a (almost long) lapse of time the drops relax and lose their gained self-assembled pattern. Figure 3(g) shows an image after four days from the start of the cooling process, where the casual re-arrangement of LC drops can be observed. At this point, the sample is re-utilizable, meaning that a new heating would lead to a new fragmentation, a new droplets coalescence and so on.

If the PDMS layer is deposited onto the Z+ face of the PPLN crystal (sample B) an opposite behavior is obtained, demonstrating that the phenomena are driven by the sign of the pyroelectric charge. After the fragmentation process the tiny droplets will coalesce again but this time the resulting LC droplets move *onto* the hexagons and remain trapped there for some hours, as shown in **Figure 4**. In this case the direction of the LN crystal dipoles is inverted into the hexagons, with respect to the case of sample A (see Figure 2). As also shown in Movie 2 (first frame in Figure 4(a)), LC droplets move and remain trapped onto hexagons, attracted in this case from the tail of the dipole arrow. The first frame of a movie (Movie 3) describing the path of single droplets is reported in Figure 4(b). The coalescence of small droplets into bigger ones, while migrating onto the center of the hexagonal domain can be observed. 19 hours after the beginning of the cooling process, the situation is that of Figure 4 (c), with the coalesced drops still present onto the hexagons. Figure 4(d) is taken under crossed polarizers, thus putting in evidence the birefringent nature of liquid crystals. In Figure 4(e), a time of the experiment corresponding more or less to Figure 4(c) is depicted.

The phenomenon at the basis of this experimental behavior is the well-known dielectrophoresis, widely described in literature.[57–67] In this case, however, the process is not induced by an external electric field, but it is due to a pyroelectric effect. So in this case we speak of pyro-electrophoretic effect, already described in,[68] but with different samples. The advantage of using liquid crystals, in this case, is the birefringent behavior of these materials and their well-known ability to change the polarization of the incident polarized light and, consequently, the huge technological impact they have.

The basis of the phenomenon is, as said above, the pyroelectric effect in PPLN.[69,70] When temperature T is constant, i.e. $\Delta T = 0$, there is no variation in the polarization P of the crystal, since the surface charges compensate that of the crystal, resulting on the whole neutral. If vice versa T increases (or decreases), the polarization decreases (or increases) consequently, and surface un-compensated charges arise. So a non-negligible electric field is generated onto the crystal surface.

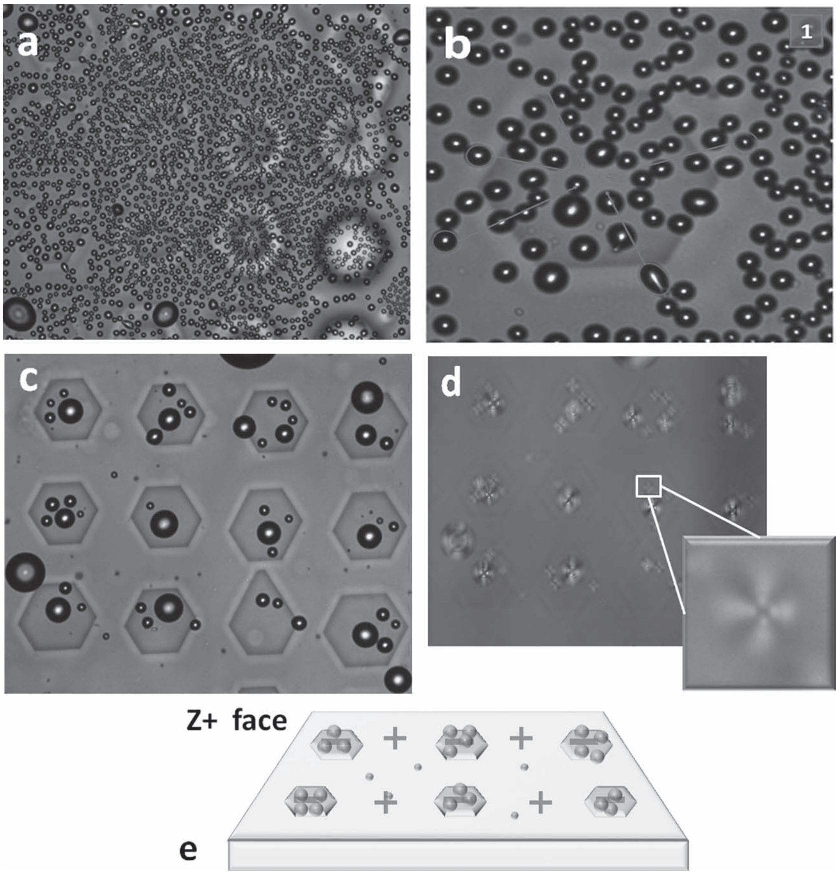

Figure 4. Experiment performed on sample B. (a) Starting frame of Movie 2 where the sample is heated at 90 °C and then cooled at room temperature for one hour. (b) First frame of Movie 3: the trajectory of five LC droplets during 62 minutes of sample cooling is monitored. (c) The sample 19 hours later, at room temperature, and (d) under crossed polarizers: Maltese crosses are well visible. (e) Scheme of the experiment.

Let's now suppose the surface of the crystal is Z- and consider the case $\Delta T < 0$, i.e. a cooling situation. As observed before, in this case LC droplets are repulsed by inverted domains (hexagons) and place themselves among them, forming a sort of matrix, as schematized in Figure 3(e). The LC molecules are repulsed from a positive charged region. Vice versa, if the surface under consideration is Z+, LC droplets are attracted by hexagons (in this case negative regions), as depicted in Figure 4(e). This behavior has to be ascribed to the strong dipole moment of the 6CHBT liquid crystal molecule.[49] In fact, analysis of electrostatic potential distribution shows that the head of the molecule exhibits negative potential, while the edges of the aromatic ring have a positive potential. The potential of the rest of the hydrocarbon chain is roughly neutral.[49]

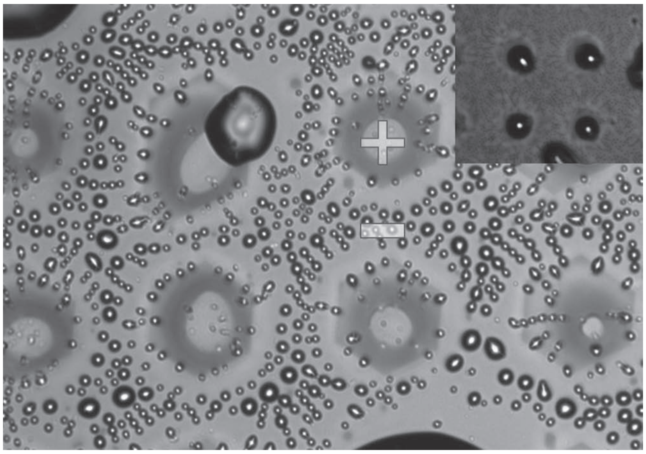

Figure 5. Microscope image of sample C cooled for 1 hour (in the LC's plane). The domains charges' signs are indicated (Z- face of the crystal). Inset: same image but in the lenses focus plane.

The situation is analogous with samples C and D. In these cases, however, arrays of PDMS microlenses, that can be activated using the pyro-electrophoretic effect, are present (see Figure 2). As an example, **Figure 5** reports an image of sample C one hour after fragmentation (i.e. after heating). Sample D (PDMS microlenses on LN Z+ face) exhibits a behavior similar to that of sample B, as expected. **Figure 6**(a-b) shows the fragmentation of LC drops after heating and their migration onto microbumps. After one hour, the situation is again similar to that of Figure 4(c), but this time the resulting effect is a single drop of LC on each microbump. In case, this latter phenomenon could be exploited to obtain self-arrangement of small LC lenses. In fact, the coalesced LC drop produces a lens effect (Figure 6c), although smaller than that produced by the PDMS bump (Figure 6d).

In the case of sample D, the droplets fragmented pattern occurring after heating is not randomly distributed, as it is for sample A (see Figure 3(b-c). In fact, as reported in Figures 6(a-b), LC droplets are aligned along radial directions passing through the center of each hexagonal domain. The geometrical arrangement suggests the fragmented drops are aligned along the lines of the electric field components in the plane of the substrate, and travel onto the domain following these lines (in analogy with the phenomenology described in Movie 3 for sample B). **Figure 7**(a-b) represents this situation, while Figure 7(c) and (d) show a close-up of Figures 6(b-c), respectively, in order to appreciate the lines formed by the LC droplets and their successive migration to the center of the domain.

3. Conclusions

In summary, many different effects of 6CHBT nematic liquid crystal droplets on periodically poled lithium niobate crystals covered with PDMS polymer, subject to a pyroelectrically generated electric field, are reported in this paper.

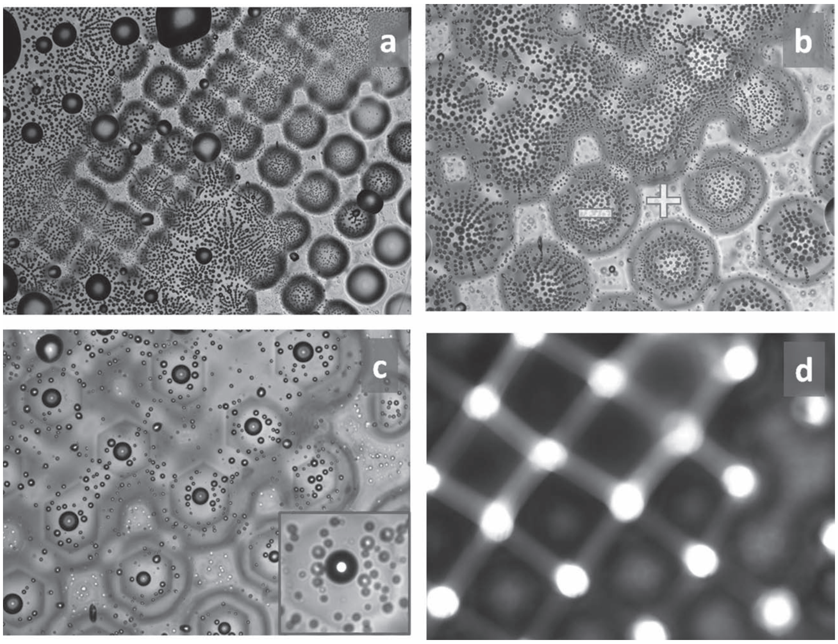

Figure 6. (a-b) Microscope images of sample D few instants after heating (Z+ side of the crystal). The fragmented droplets are onto hexagonal domains (with negative charges), according to the previous measurements. (c-d) Images of the sample one hour later (i.e. after one hour of cooling): (c) in the LC's plane and (d) in the PDMS lenses focal plane. Inset of (c): image in the LC lens' focal plane.

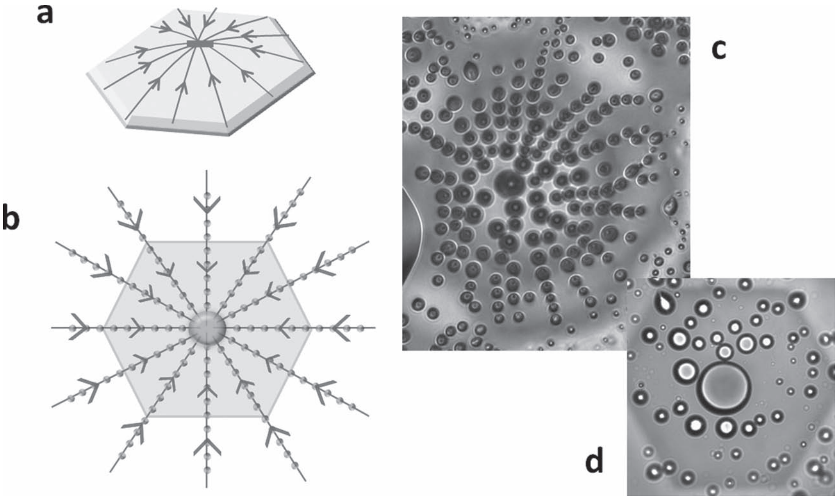

Figure 7. (a) Side and (b) top view of the electric field lines pyroelectrically generated, going from the positive charges (around hexagons) to the negative (onto hexagons). (c-d) Microscope images of one hexagonal domain of sample D (c) few seconds after heating and (d) one hour later.

We observed fragmentation effects of drops in smaller ones, migration to different regions of the sample according to the geometry of the lithium niobate substrate (pyro-electrophoretic effect) and following the electric field lines, successive coalescence in bigger drops with the possibility of new fragmentation (reversibility of the process), square-matrix arrangements and lens effects, and planar alignment of the liquid crystal directors (Maltese crosses).

This novel approach for manipulating liquid crystals by pyroelectric effect, where the strong electric fields generated through a thermal stimulus allow to manipulate liquids in 2D on a substrate, can be suitable for applications such as spatial modulation of the wettability (i.e. wettability patterning), or, in principle, a dynamical optical element able to switch from a diffuser state (fragmentation) to a microlens array (coalescence state). In case, the birefringent microlenses could be also tunable. Of course, the coalescence effect should be helped by an appropriate micropatterning of the substrate allowing to have coalescence in fixed locations.

4. Experimental Section

Samples preparation: A polished 500-μm-thick LN z-cut crystal (Crystal Technology Inc.) is subject to conventional mask-photolithography and standard periodic electric field poling in order to achieve a square array of hexagonal reversed domains.[71,72] An external voltage, exceeding the coercive field of the material (around 21 kV/mm), is necessary to reverse the ferroelectric domains; the inversion selectivity is ensured by an appropriate resist pattern, generated by conventional photolithography. The period of the obtained domains is around 200 μm along both x and y crystal directions.[69] Different samples have been prepared by covering the PPLN samples with thin layers of polydimethylsiloxane (PDMS) polymer solution (Dow Corning Sylgard 184, 10:1 mixing ratio base to curing agent), spin-coated at 6000 RPM for 2 minutes. Experiments are performed by using both sides of the PPLN samples, Z- and Z+. We have prepared samples with thin and uniform layer of PDMS and samples with micro patterned PDMS microbumps structures,[31–33] that are also useful as an array of microlenses. The whole process to obtain this PDMS solid structures is described in detail in.[33] As schematized in Figure 2, samples A and B consist of a homogeneous thin layer of PDMS spin-coated on the Z- (A) and Z+ (B) face of the LN substrate, while samples C and D are placed onto a hotplate at a temperature of 170 °C for 30s, thus inducing the formation of PDMS microlenses (on Z- and Z+ respectively), following the arrangement of the hexagonal domains.[31–33]

Supporting Information

Supporting Information is available from the Wiley Online Library or from the author.

Received: February 6, 2012
Revised: March 6, 2012

---

[1] G. Gibson, D. M. Carberry, G. Whyte, J. Leach, J. Courtial, J. C. Jackson, D. Robert, M. Miles, M. Padgett, *J. Opt. A: Pure Appl.*

Opt. **2008**, *10*, 044009.
[2] T. H. Kim, Y. W. Lee, I. W. Lee, S. C. Choi, *Appl. Opt.* **2000**, *39*, 2054.
[3] T. Yamada, A. Suzuki, N. Uchiyama, N. Ohuchi, S. Takahashi, *Eur. Radiol.* **2008**, *18*, 2363.
[4] P. Jägemalm, L. Komitov, G. Barbero, *Appl. Phys. Lett.* **1998**, *73*, 1616.
[5] A. Fratalocchi, R. Asquini, G. Assanto, *Opt. Express* **2005**, *13*, 32.
[6] J. A. Davis, G. H. Evans, K. Crabtree, I. Moreno, *Appl. Opt.* **2004**, *43*, 6235.
[7] Y. J. Kim, M. R. Luo, W. Choe, H. S. Kim, S. O. Park, Y. Baek, P. Rhodes, S. Lee, C. Y. Kim, *J. Opt. Soc. Am. A* **2008**, *25*, 2215.
[8] W.-H. Su, C.-H. Hsu, W.-C. Su, J.-P. Liu, *Opt. Express* **2011**, *19*, 3272.
[9] U. Efron, S. T. Wu, T. D. Bates, *J. Opt. Soc. Am. B* **1986**, *3*, 247.
[10] H. T. Dai, Y. J. Liu, X. W. Sun, D. Luo, *Opt. Express* **2009**, *17*, 4317.
[11] H. Ren, D. W. Fox, B. Wu, S.-T. Wu, *Opt. Express* **2007**, *15*, 11328.
[12] M. Ye, B. Wang, S. Sato, *Appl. Opt.* **2004**, *43*, 6407.
[13] H. Ren, S.-T. Wu, *Opt. Express* **2006**, *14*, 11292.
[14] M. Humar, M. Ravnik, S. Pajk, I. Musevic, *Nat. Phot.* **2009**, *3*, 595.
[15] E. Nagali, L. Sansoni, F. Sciarrino, F. De Martini, L. Marrucci, B. Piccirillo, E. Karimi, E. Santamato, *Nat. Phot.* **2009**, *3*, 720.
[16] Z. Ghattan, T. Hasek, R. Wilk, M. Shahabadi, M. Koch, *Opt. Commun.* **2008**, *281*, 4623.
[17] Y. Yuan, J. He, J. Liu, J. Yao, *J. Phys.: Conf. Series* **2011**, *276*, 012228.
[18] H. Zhang, P. Guo, P. Chen, S. Chang, J. Yuan, *J. Opt. Soc. Am. B* **2009**, *26*, 101.
[19] S. V. Kalinin, D. A. Bonnell, *Phys. Rev. B* **2001**, *63*, 125411.
[20] G. I. Distler, V. P. Konstantinova, Y. M. Gerasimov, G. A. Tolmacheva, *Nature* **1968**, *218*, 762.
[21] S. Dunn, D. Cullen, E. Abad-Garcia, C. Bertoni, R. Carter, D. Howorth, R. W. Whatmore, *Appl. Phys. Lett.* **2004**, *85*, 3537.
[22] S. Habicht, R. J. Nemanich, A. Gruverman, *Nanotech.* **2008**, *19*, 495303.
[23] B. J. Rodriguez, R. J. Nemanich, A. Kingon, A. Gruverman, S. V. Kalinin, K. Terabe, X. Y. Liu, K. Kitamura, *Appl. Phys. Lett.* **2005**, *86*, 012906.
[24] J. L. Giocondi, G. S. Rohrer, *Chem. Mater.* **2001**, *13*, 241.
[25] S. V. Kalinin, D. A. Bonnell, T. Alvarez, X. Lei, Z. Hu, J. H. Ferris, Q. Zhang, S. Dunn, *Nano Lett.* **2002**, *2*, 590.
[26] D. Ehre, E. Lavert, M. Lahav, I. Lubomirsky, *Science* **2010**, *327*, 672.
[27] J. N. Hanson, B. J. Rodriguez, R. J. Nemanich, A. Gruverman, *Nanotech.* **2006**, *17*, 4946.
[28] Y. Sun, R. J. Nemanich, *J. Appl. Phys.* **2011**, *109*, 104302.
[29] A. Haussmann, P. Milde, C. Erler, L. M. Eng, *Nano Lett.* **2009**, *9*, 764.
[30] M.-P. Bernal, J. Amet, J. Safioui, F. Devaux, M. Chauvet, J. Salvi, F. I. Baida, *Appl. Phys. Lett.* **2011**, *98*, 071101.
[31] P. Ferraro, S. Grilli, L. Miccio, V. Vespini, *Appl. Phys. Lett.* **2008**, *92*, 213107.
[32] F. Merola, M. Paturzo, S. Coppola, V. Vespini, P. Ferraro, *J. Micromech. Microeng.* **2009**, *19*, 125006.
[33] S. Grilli, L. Miccio, V. Vespini, A. Finizio, S. De Nicola, P. Ferraro, *Opt. Express* **2008**, *16*, 8084.
[34] Y.-J. Lee, Y. W. Kim, Y.-K. Kim, C.-J. Yu, J. S. Gwag, J.-H. Kim, *Opt. Express* **2011**, *19*, 10673.
[35] P. Ferraro, S. Coppola, S. Grilli, M. Paturzo, V. Vespini, *Nat. Nanotech.* **2010**, *5*, 429.
[36] S. Grilli, S. Coppola, V. Vespini, F. Merola, A. Finizio, P. Ferraro, *Proc. Natl. Acad. Sci.* **2011**, *108*, 15106.
[37] S. C. Bharath, K. R. Pimputkar, A. M. Pronschinske, T. P. Pearl, *Appl. Surf. Sci.* **2008**, *254*, 2048.
[38] Z. Zhang, P. Sharma, C. N. Borca, P. A. Dowben, A. Gruverman, *Appl. Phys. Lett.* **2010**, *97*, 243702.
[39] S. Tonini, M. Gavaises, A. Theodorakakos, *Intern. Journ. Therm. Scien.* **2009**, *48*, 554.
[40] Y. Renardy, V. Cristini, J. Li, *Intern. Journ. Multiph. Flow* **2002**, *28*, 1125.
[41] E. Villermaux, *Annu. Rev. Fluid Mech.* **2007**, *39*, 419.
[42] Y. Y. Renardy, V. Cristini, *Phys. Fluids* **2001**, *13*, 2161.
[43] K. Ichiki, S. Consta, *J. Phys. Chem. B* **2006**, *110*, 19168.
[44] O. Sotolongo-Costa, Y. Moreno-Vega, J. J. Lloveras-González, J. C. Antoranz, *Phys. Rev. Lett.* **1996**, *76*, 42.
[45] B. Sun, J. Heikenfeld, *J. Micromech. Microeng.* **2008**, *18*, 025027.
[46] I. Viola, M. Mazzeo, A. Passabì, S. D'Amone, R. Cingolani, G. Gigli, *Adv. Mater.* **2005**, *17*, 2935.
[47] S. Herminghaus, K. Jacobs, K. Mecke, J. Bischof, A. Fery, M. Ibn-Elhaj, S. Schlagowski, *Science* **1998**, *282*, 916.
[48] B. D. Hamlington, B. Steinhaus, J. J. Feng, D. Link, M. J. Shelley, A. Q. Shen, *Liquid Crys.* **2007**, *34*, 861.
[49] M. Szaleniec, R. Tokarz-Sobieraj, W. Witko, *J. Mol. Model.* **2009**, *15*, 935.
[50] R. B. Bogoslovov, C. M. Roland, J. Czub, S. Urban, *J. Phys. Chem. B* **2008**, *112*, 16008.
[51] Y.-P. Chiu, C.-Y. Shen, W.-C. Wang, T.-Y. Chu, Y.-H. Lin, *Appl. Phys. Lett.* **2010**, *96*, 131902.
[52] L. Valentini, F. Mengoni, A. Taticchi, A. Marrocchi, J. M. Kenny, *J. Mater. Chem.* **2006**, *16*, 1622.
[53] F. Mugele, J.-C. Baret, *J. Phys.: Condens. Matt.* **2005**, *17*, R705.
[54] F. Vandenbrouck, M. P. Valignat, A. M. Cazabat, *Phys. Rev. Lett.* **1999**, *82*, 2693.
[55] J. Heikenfeld, M. Dhindsa, *J. Adhes. Sci. and Tech.* **2008**, *22*, 319.
[56] P. K. Rai, M. M. Denn, C. Maldarelli, *Langmuir* **2003**, *19*, 7370.
[57] P. Mokrý, M. Marvan, J. Fousek, *J. Appl. Phys.* **2010**, *107*, 094104.
[58] H. Pohl, *J. Appl. Phys.* **1951**, *22*, 869.
[59] I.-F. Cheng, H.-C. Chang, D. Hou, H.-C. Chang, *Biomicrofluidics* **2007**, *1*, 021503.
[60] S. Liu, J. B.-H. Tok, J. Locklin, Z. Bao, *Small* **2006**, *2*, 1448.
[61] B. Weiss, W. Hilber, R. Holly, P. Gittler, B. Jakoby, K. Hingerl, *Appl. Phys. Lett.* **2008**, *92*, 184101.
[62] C. Zhang, K. Khoshmanesh, F. J. Tovar-Lopez, A. Mitchell, W. Wlodarski, K. Klantar-zadeh, *Microfluid. Nanofluid.* **2009**, *7*, 633.
[63] A. Rosenthal, J. Voldman, *Biophys. Journ.* **2005**, *88*, 2193.
[64] T. Kimura, M. Yamato, A. Nara, *Langmuir* **2004**, *20*, 572.
[65] H. A. Eggert, F. Y. Kuhnert, K. Buse, J. R. Adleman, D. Psaltis, *Appl. Phys. Lett.* **2007**, *90*, 241909.
[66] R. Cicoria, Y. Sun, *Nanotech.* **2008**, *19*, 485303.
[67] K.-L. Cheng, Y.-J. Sheng, S. Jiang, H.-K. Tsao, *J. Chem. Phys.* **2008**, *128*, 101101.
[68] S. Grilli, P. Ferraro, *Appl. Phys Lett.* **2008**, *92*, 232902.
[69] S. Grilli, V. Vespini, P. Ferraro, *Langmuir* **2008**, *24*, 13262.
[70] E. M. Bourim, C.-W. Moon, S.-W. Lee, I. K. Yoo, *Phys. B* **2006**, *383*, 171.
[71] S. Grilli, M. Paturzo, L. Miccio, P. Ferraro, *Meas. Sci. Technol.* **2008**, *19*, 074008.
[72] S. Grilli, P. Ferraro, M. Paturzo, D. Alfieri, P. De Natale, *Opt. Express* **2004**, *12*, 1832.